Topology Optimization of Two-Degree-of-Freedom Micro-Actuator

Zhaokun Li
Engineering of mechanical and electrical department
Beijing polytechnic college
Beijing, China
2008lizhaokun@163.com

Yong Guo
Engineering of mechanical and electrical department
Beijing polytechnic college
Beijing, China
22812069@qq.com

Xiaoxue Yang
Engineering of mechanical and electrical department
Beijing polytechnic college
Beijing, China
yangxiaoxue123@hotmail.com

Huamei Bian
Engineering of mechanical and electrical department
Beijing polytechnic college
Beijing, China
bianhuamei0@163.com

Abstract—For example of the two-degree-of-freedom micro-actuator, the topology optimization, extraction and experiment are investigated. Firstly, the topology optimization model considering the suppression strategy of input and output coupling terms and optimization algorithm is developed. Secondly, according to the specific characteristics of compliant mechanisms, a topology extraction method is presented, which includes image preprocessing, boundary extraction using the density contour method, and geometric reconstruction. Finally, based on the topology mechanism and the restriction of fabrication technology, the prototype of the two-degree-of-freedom micro-actuator is determined. The prototype is fabricated by means of linear cutting technology. The displacements of the two-degree-of-freedom micro-actuator are measured by using the control system. The experimental results show that properties of the two-degree-of-freedom micro-actuator can satisfy the designing demand and this approach available.

Keywords- compliant mechanism; multiple inputs and outputs; topology extraction; experiment investigation; topology optimization

I. INTRODUCTION

In recent years, the research on the topology optimization of compliant mechanisms has made great progress [1]. But so far, a number of papers on the topology optimization of compliant mechanisms presented mostly deal with the single input and output optimization problem, the results for single input and multiple outputs optimization and for multiple inputs and outputs optimization can be seen respectively in only few references [2]. And in practical applications, multiple degree-of-freedom compliant mechanisms are widely used in the fields of micro-positioning and micro-manipulation. Meanwhile, the topology optimization of compliant mechanisms is actually a geometrically nonlinear problem. Only few papers have appeared in References [3-5], the research on multi-inputs and multi-outputs topology optimization of micro-compliant mechanisms undergoing large deformation need to further investigate.

Furthermore, the resulting image of the topology optimization is non-smooth geometric model which cannot be manufactured much more easily. And relatively high stresses are observed on specific parts of the boundaries, especially around the hinges. The control of local physical quantities such as stress in the stage of topology optimization is difficult [6]. Such disadvantage of topology optimization can be overcome to some extent by applying shape optimization to the result of topology optimization. That is, topology mechanisms must be extracted into the CAD parameter model and then be performed by shape optimizations. Up to now, the approaches of topology extraction can be roughly divided into three categories: image interpretation approach, density contour approach, and geometric reconstruction approach [7-9].

In this research, for example of the two-degree-of-freedom micro-actuator, the topology optimization, extraction and of experiment is investigated. Firstly, the topology optimization model considering the suppression strategy of input and output coupling terms and optimization algorithm is developed. Secondly, according to the specific characteristics of compliant mechanisms, a topology extraction method is presented. Finally, based on the topology mechanism and the restriction of fabrication technology, the prototype of the two-degree-of-freedom micro-actuator is determined. The prototype is fabricated by means of linear cutting technology. The displacements of the two-degree-of-freedom micro-actuator are measured by using the control system. The experimental results show that properties of the two-degree-of-freedom micro-actuator can satisfy the designing demand and this approach available.

II. TOPOLOGY OPTIMIZATION OF MULTI-INPUT AND MULTI-OUTPUT COMPLIANT MECHANISMS

Consider a general design domain Ω of multiple inputs and multiple outputs compliant mechanism with boundary and loading conditions. The springs at the output port

simulate the resistances from the work-pieces. The input loads are represented as tractions $F_i(i = 1,2,\cdots,n)$ applied at input points $I_i(i = 1,2,\cdots,n)$ and the output displacements $u_{out,j}(j = 1,2,\cdots,n_0)$ at output points $O_j(j = 1,2,\cdots,n_0)$ along the desired directions should be maximized. Where n and n_0 respectively is numbers of multi-input and multi-output, $k_{out,j}$ is output simulated stiffness.

The system flexibility requirement is met by maximizing Geometric Advantage [3, 4]. This is achieved by maximizing the ratio of the output displacement $(u_{out,j})$ over the input displacement $(u_{in,i})$. If input displacements are constrained, this is equivalent to maximizing $u_{out,j}$ and for the case of multiple output requirements the formulation extensively is defined as:

$$\max \quad u_{out} = \sum_{j=1}^{n_0} u_{out,j} \qquad (1)$$

The need for the compliant mechanism to be stiff enough to withstand the external load is captured as the stiffness requirement [3, 4]. The stiffness of the mechanisms with boundary and loading conditions is now considered.

Maximizing stiffness requirement is determined by minimizing Strain Energy (S_E) which is equivalent to minimizing mean compliance (P) of the structures and the formulation is defined as:

$$\min S_E \Leftrightarrow \min P = F^T U \qquad (2)$$

Where U is the displacement vector, F is the sum of all the external forces.

The input and output coupling effect of compliant mechanisms should be suppressed when mechanism maneuverability requires more accurately. That is, some output displacement responses are expected more sensitive to one specified input force than that of the other [1]. In order to illustrate the corresponding relationship between the input load and the output displacement, the output displacements $u_{out,j}$ can be substituted as $u_{out,i,j}$ meaning that corresponding to the input ports I_i at specified output points O_j along the desired directions. So equation (1) can be further developed as:

$$u_{out} = \sum_{j=1}^{n_0} u_{out,j} = \sum_{i=1}^{n}\sum_{j=1}^{n_0} u_{out,j} = \sum_{i=1}^{n} u_{out,i,i} + \sum_{i=1}^{n}\sum_{\substack{j=2\\j\neq i}}^{n_0} u_{out,i,j} \quad (3)$$

where

$$u_{out1} = \sum_{i=1}^{n} u_{out,i,i} \quad, \quad u_{out2} = \sum_{i=1}^{n}\sum_{\substack{j=2\\j\neq i}}^{n_0} u_{out,i,j}$$

The topology optimization of compliant mechanisms is a multiobjective problem. And so far, there are many approaches to generate solutions, and most of solution sachems transform the multiple objectives into a single objective [10]. Based on the modified norm method, a scalar optimization problem is used and the formulation is defined as:

$$f(x) = \sum_i w_i f_i(x) h_i \qquad (4)$$

Where $f_i(x)$ is the ith objective function, x represents a design variable vector, w_i is the weighting coefficient for the ith objective and h_i is the constant multiplier which make each objective function have the dimensionless value of the same order.

Using the SIMP approach, the relative density x_e of material in each element is a design variable. The N-vector containing the design variables is denoted x. The overall multiobjective topology optimization solving the problem of distributing a limited amount of material in the design domain such that the multiobjective function for the multiple inputs and outputs compliant mechanisms is minimized and the volume and input displacement is constrained can be expressed as:

$$\min_{x_e} f(x) = w_1(P/P_0) - w_2(u_{out1}/u_{01}) +$$
$$(1 - w_1 - w_2)(u_{out2}/u_{02})$$
$$\text{Subject to:} \quad R = 0 \qquad (5)$$
$$V^T x \leq V^*$$
$$0 < x_{min} \leq x_e \leq 1$$
$$u_{in}(x_e) \leq u_{in}^*$$

where P_0 represent the mean compliance , u_{01} and u_{02} represent the output displacement of the uniformly perforated initial structure, respectively, V is N-vector containing the element volume, V^* is the upper bound on material volume and x_{min} is an N-vector with the minimum values of the densities and R denotes the inner and external force vectors.

The large-deflection equilibrium is solved using Newton-Raphson iteration scheme. The optimization problem is solved using the MMA method proposed, the sensitivity analysis and the multiobjective topology optimization of multi-input and multi-output compliant mechanisms with geometrically nonlinearity is referenced as [10].

III. TOPOLOGY EXTRACTION PROCESS

Topology extraction process consists of image preprocessing, boundary extraction and the B-spline curve reconstruction.

A. Topology extraction process

Topology grey image of at the specific condition and cannot be manufactured [7]. The grey level image must be converted to a binary of equal density. Topology grey image converted to a binary image needs a threshold value T and it can be done by redefining material densities zero in elements where densities are less than the threshold value T. And elements with densities greater than the threshold value T will be redefined as elements with densities equal to 1.

Compared with the traditional image processing, the topology algorithm of image post-processing should consider not only the smoothness of structure image, but also the initial topology objective function. The design domain of in figure 1 reduces material to 30 percent considering stiffness constant in the topology optimization, then in the subsequent post-processing of the image object

will maintain invariant. Corresponding relationship between design variables x_i and the gray level ρ_i is expressed as: $\rho_i = x_i \rho_0$, that is, deducing to grey image volume sum equal to the gray level: $V_i = x_i V_0$, then in the subsequent post-processing of the image object will maintain volume invariant. The difference of the grey sum fore and after binary image processing is expressed as:

$$\Delta V = \sum f(x,y) - \sum g(x,y) \qquad (6)$$

Then the optimal threshold selection T^* must satisfy this condition $\Delta V = 0$. Because ΔV is of the monotone decreasing function of the threshold T, the optimal threshold T^* is determined by dichotomy. Postulating initial values T_1, T_2 are the respectively minimum and maximum values of image gray, and the basic algorithm is as follows:

1) postulating $T = (T_1 + T_2)/2$;

2) structure image binary, calculating ΔV, if $\Delta V > 0$, then $T_1 = T$, if $\Delta V < 0$, then $T_2 = T$;

3) if $|T_2 - T_1| < \varepsilon$, ε is the degree of convergence, loop ends; else, from the beginning of 1);

4) Obtain the optimal threshold $T^* = T$。

This example considers only a single constraint condition of the volume, and binary image is shown as in Fig 1. (b). For the two constraint conditions and the three constraints which satisfy the maximum output displacement, the volume and minimum mean compliance constraints respectively using different threshold density values starting from 0.1 to 1, with increment 0.1. To obtain the final proper threshold, one threshold is achieved firstly satisfying one objective function, and then calculating multi-objective threshold using weighted superposition. Multiobjective topology extraction of multi-input and multi-output compliant mechanisms is referenced as [11].
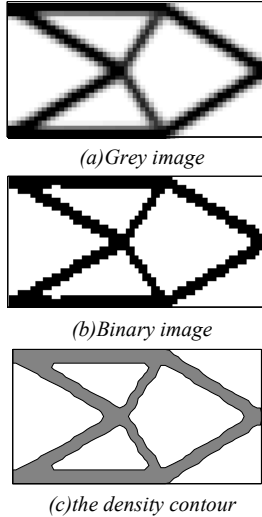

(a)Grey image

(b)Binary image

(c)the density contour

Figure1. A typical example of structure topology evolution

B. The density contour approach

To generate the smooth boundaries, the density contour approach [8] is used. In this works, the element densities of topology optimization result are redistributed into nodal densities, and the nodal density contour is generated at a specified density value. Averaging the normalized material densities of the neighboring elements are followed as:

$$\rho_k = \frac{1}{M} \sum_{e=1}^{M} \rho_{k,e} \qquad (7)$$

Where, ρ_k is the density of the k-th node, M is the number of neighboring elements at this node, $\rho_{k,e}$ is the normalized material density of the e-th neighboring element of the k-th node. In two dimensional topology optimization, almost all nodes have four neighboring elements, and thus $M = 4$. The climax points and boundary points are needed special calculation. The node density of three cases can be expressed as follows:

$$\begin{cases} \rho_1 = \rho^1 & \text{climax point} \\ \rho_2 = 1/2(\rho^1 + \rho^2) & \text{boundary point} \\ \rho_6 = 1/4(\rho^1 + \rho^2 + \rho^4 + \rho^5) & \text{generals} \end{cases} \quad (8)$$

There are three possibilities of nodal density values using Equation (12), $\rho_k = 0$, $\rho_k = 1$ and $0 < \rho_k < 1$. Fig1(c) shows the nodal density contour of the examples using the density contour approach.

C. The B-spline curve reconstruction

The approximate nodal density contour is parameterized by using B-spline curves. The B-spline curve with the (k-1) th order polynomial blending functions is expressed as [9, 12]:

$$x(u) = \sum_{i=0}^{n} B_i N_{i,k}(u) \qquad (9)$$

where the blending function $N_{i,k}(u)$ is recursively defined as :

$$\begin{cases} N_{i,1}(u) = \begin{cases} 1 & t_i \le u \le t_{i+1} \\ 0 & otherwise \end{cases} \\ N_{i,k}(u) = \dfrac{(u - t_i)N_{i,k-1}(u)}{t_{i+k-1} - t_i} + \dfrac{(t_{i+k} - u)N_{i+1,k-1}(u)}{t_{i+k} - t_{i+1}} \end{cases} \quad (10)$$

In Eq. (9), B_i means the control point, and t_i in Eq. (5) is the knot value.

The approximated boundaries with B-spline curves for shape optimization are obtained by minimizing:

$$f = \sum_{j=0}^{r} \left\| P_j - x(u_j) \right\|^2 \qquad (11)$$

where P_j denotes the smoothed boundary known point.

The values of u_j are determined by

$$\begin{cases} u_0 = 0 \\ u_j = u_{j-1} + \dfrac{l_j}{L}, r = 1,...,j \\ l_j = \left| P_j - P_{j-1} \right| \\ L = \sum_{i=1}^{r} l_j \end{cases} \quad (12)$$

To minimize Eq. (12), the derivatives of f with respect to n + 1 control points are set to be zero: $\frac{\partial f}{\partial B_l} = 0$, and establishing equation:

$$\frac{\partial f}{\partial B_l} = 0 \ (l = 0,1,\cdots,n)$$

$$\frac{\partial f}{\partial B_l} = \sum_{j=0}^{r} \left\| -2P_j \sum_{i=0}^{n} N_{i,k}(u_j) + 2\sum_{i=0}^{n} N_{i,k}(u_j) \left(\sum_{i=0}^{n} N_{i,k}(u_j) B_l \right) \right\| = 0 \tag{13}$$

According to Eq. (13), the following matrix equation is leaded:

$$N^{\mathrm{T}} N B = N^{\mathrm{T}} P \tag{14}$$

Where

$$N = \begin{bmatrix} N_{0,k}(u_0) & N_{1,k}(u_0) & \cdots & N_{n,k}(u_0) \\ N_{0,k}(u_1) & N_{1,k}(u_1) & \cdots & N_{n,k}(u_1) \\ \cdots & \cdots & \cdots & \cdots \\ N_{0,k}(u_r) & N_{1,k}(u_r) & \cdots & N_{n,k}(u_r) \end{bmatrix}_{(r+1)\times(n+1)}$$

According to equation (14),

$$B_{(n+1)*k} = \left(N^T N \right)^{-1}_{(n+1)*(n+1)} N^T_{(n+1)*(r+1)} P_{(r+1)*k} \tag{15}$$

Where B and P denote the vectors of control points and smoothed boundary points, respectively. The coordinates of the control points and the widths of the hinges are regarded as design variables in fig.1 during the shape optimization not all the control points.

IV. NUMERICAL EXAMPLES

A. Topology optimization of the two-degree-of-freedom micro-actuator

Fig.2 shows the design domain of the compliant mechanism with two inputs and two outputs. The dimension of the design domain, the material properties, and the input parameters for the optimization program are shown in Table 1.
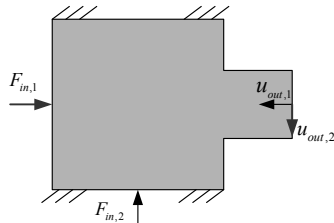

Figure2. Design domain of topology optimization for 2D actuator

Table1. Input parameters of topology optimization

Variable name	Setting value	Variable name	Setting value
Design domainS_j/mm	70×50	Input spring stiffness $k_{in,i}$/N · mm^{-1}	0.1
Input force 1 F_i/N	1	output spring stiffness $k_{out,j}$/N · mm^{-1}	0.1
Crippling size D/mm	20×20	Poisson ratio V	0.3
Young modulu E/Gpa	100	V/V_0	0.3

Firstly, the single objective optimization are executed to find P_0 and u_0. Table2 (a) and (b) shows the optimal topology of the stiffness optimization and the flexibility optimization, respectively. The best compromise design is found in the case of $w = 0.3$ based on the decision function [15]. Table2 exhibits significant difference from the single objective optimization.

Secondly, the overall multiobjective topology optimization function considering the suppression strategy of input and output coupling terms is studied. The output coupling displacements without considering coupling terms suppression in the case of $w = 0.3$ are much larger than that with considering coupling terms suppression in the case of $w_1 = 0.3$ and $w_2 = 0.6$ under the same applied force shown in Table 3, it goes without saying that the presented suppression strategy of input and output coupling terms of exhibits the validity.

Table2. Geometrical features of topology optimization of the two-degree-of-freedom micro-actuator

a) Stiffness problem	
b) flexibility problem	
c) Multiobjective optimal in the case of $w = 0.3$	
d) Linear mechanism with coupling terms suppression	
e) Nonlinear mechanism with coupling terms suppression	

Table 3. Comparisons of output displacement with and without output coupling terms suppression

Displacement and displacement ratio	Without output coupling terms suppression	With output coupling terms suppression
Output displacement corresponding to input1 $u_{out,1,1}$/μm	31.58	31.35
Coupling output displacement at the output point 2 $u_{out,2,1}$/μm	13.18	1.20
Displacement ratio $u_{out,2,1}/u_{out,1,1}$	0.42	0.04
Coupling output displacement at the output point 1 $u_{out,1,2}$/μm	14.58	3.69
Output displacement corresponding to input 2 $u_{out,2,2}$/μm	35.66	36.34
Displacement ratio $u_{out,1,2}/u_{out,2,2}$	0.41	0.11

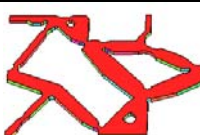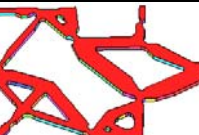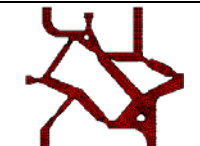**Table 4.** Results Comparison of linear and nonlinear design
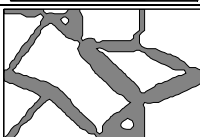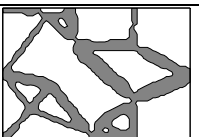
|	Output displacement corresponding to input1$u_{out,1,1}$/μm	Output displacement corresponding to input2$u_{out,2,2}$/μm	Mean compliance **P**/F.μm
Linear design	22.38	31.13	26.29
Nonlinear design	31.35	36.34	23.43

Finally, comparing the linear finite element analysis topology with the nonlinear one, The linear topology optimization is carried out and the result is illustrated in Table3 (d). The nonlinear result obtained from the proposed method is shown in Table3 (e), which exhibits significant difference from the linear one. The output displacement and the compliance values of the linear design and the nonlinear one with coupling terms control in the case of $w_1 = 0.3$ and $w_2 = 0.6$ are summarized in Table 4. It can be seen that the nonlinear design experiences much larger output displacements and smaller compliances, which illuminates that the use of the multiobjective topology optimization with geometrically nonlinearity can improve the performance of a compliant mechanism.

B. topology extraction and finite element analysis

The topology extraction is executed for considering coupling and without coupling terms suppression .The topology extraction procedure is shown in Table5.

Table 5. Linear and nonlinear topology mechanism

	Linear	nonlinear
(a)topology optimization		
(b)binary image		
(c)density contour		
(d)CAD modal		
(e)Optimized CAD modal		

(f)simulation deformation	
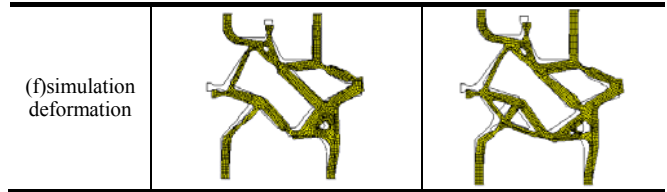
Based on optimization results, a two-dimensional micro-actuator by piezoelectric ceramic actuator as the driving source, considering the maximum input force, strength, geometric as well as the output coupling constraints, the parameters of the compliant hinge is optimized and the optimized model is shown in Table 5 (e). The extraction mechanisms of linear and nonlinear are designed as shown in Fig.3.

In order to sort out which design is better, the mechanical deformations are calculated using Ansys software. Its Young modulus is 210Gpa and its Poisson ratio is 0.3 . Table 5 (f) shows the deformations of the linear design and the nonlinear design, respectively. The output displacements of nonlinear design is $21.811 \mu m$ and the linear one is $16.606 \mu m$ when the input displacement is $20 \mu m$. It can be seen that the nonlinear design experiences larger deformation under the same applied force. The stress distributions of the two mechanisms illuminates that the maximum stress of the nonlinear topology is 133.85Mpa, much smaller than that of the linear one which is153.109Mpa. The importance of using nonlinear finite element analysis is clearly demonstrated by this example.
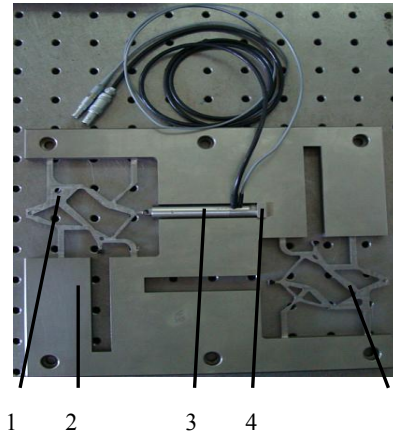

1. Linear mechanism; 2.main mechanism3; piezoelectric ceramic actuator；4．Positioning wedge；5．Nonlinear mechanism
Figure3. Photography of 2D actuator

C. Displacement measurement

Based on the topology mechanism and the restriction of fabrication technology, the prototype of the two-degree-of-freedom micro-actuator is determined as shown in Fig.3, the prototype is fabricated by means of linear cutting technology. The size of the precision positioning platform is $230mm \times 200mm \times 12mm$, the main micro-actuator thickness is$1.5mm$. The type of the piezoelectric ceramic actuator is PZT as shown in Fig. 3(3) .The displacements of the two-degree-of-freedom micro-actuator are measured by using the control system as shown in Fig.4.

Fig.6 illustrates the results comparison of finite element analysis and experiment for the linear design and the nonlinear one. The output displacement of nonlinear design is19.771 μm and the linear one is 15.192 μm when the input displacement is $20 \mu m$. It can be seen that the nonlinear design experiences larger deformation, and from which it is noted that the linear traces of the simulation and measurement take on linear trend, but also the nonlinear traces presents curvilinear trend with rapid of input displacement. The experimental results show that properties of the two-degree-of-freedom micro-actuator can satisfy the designing demand.
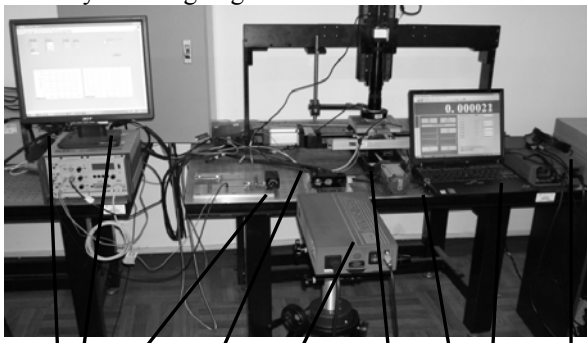
1. Industrial Personal Computer; 2.computer; 3.micro-actuator; 4.interferoscope;5.laser interferometer; 6.reflecting mirror; 7. Newport shock isolation system; 8. computer2 ; 9. Compensator
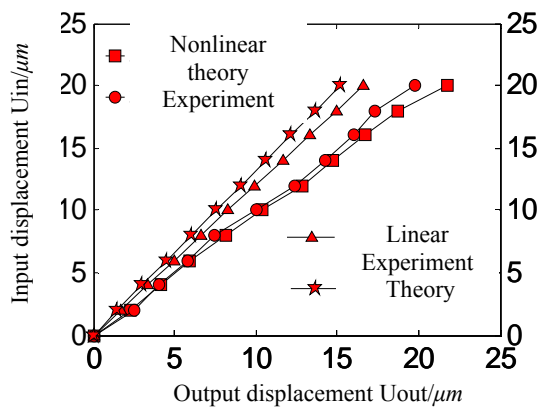Figure4.Hardware platform of the computer displacement system

Figure6. Results of Input and output displacement relation

V. CONCLUSIONS

For example of the two-degree-of-freedom micro-actuator, this paper illustrates the overall process from topology optimization of multi-degree-of-freedom compliant mechanisms to topology extraction and experiment investigation.

The results of numerical example are presented to show that (1) the suppression strategy of input and output coupling terms presented for multiple inputs and outputs compliant mechanisms is correct and the geometrically nonlinear finite element analysis is necessary to find the optimal design of the large displacement micro-compliant mechanisms;(2) The binary transaction, the density contour smoothness and the B-spline curves reconstruction applied on the example show that income mechanisms meet to project practice; (3) the simulated deformation results of finite element analysis after topology extraction, comparing to topology optimization results basely meet the challenge; (4)The prototype is fabricated by means of linear cutting technology. The displacements of the two-degree-of-freedom micro-actuator are measured by using the control system. The experimental results show that properties of the two-degree-of-freedom micro-actuator can satisfy the designing demand and this approach available.

REFERENCES

[1] Zhang Xian-min, Topology optimization of compliant mechanisms, Chinese journal of mechanical engineering, 2003, 39(11), pp. 47-51. (In Chinese)

[2] Frecker M I, Kikuchi N, Kota S．Topology optimization of compliant mechanisms with multiple outputs[J]．Structural Optimization, 1999, 17(4): 269-278.

[3] Pedersen C B W, Buhl T, Sigmund O. Topology synthesis of large-displacement compliant mechanisms [J]．International Journal for Numerical Methods in Engineering, 2001, 50(12): 2683–2705.

[4] Sigmund O．Design of multiphysics actuators using topology optimization—Part I: one-material structures[J]．Computer Methods in Applied Mechanics and Engineering, 2001, 190(49-50): 6577-6604.

[5] Gea H C, Luo J H．Topology optimization of structure with geometrical nonlinearities[J]. Computers and Structures, 2001, 79(20-21): 1977-1985．

[6] Duysinx P., Bendsoe M.P．Topology optimization of continuum structures with local stress constraints[J].International journal for numerical methods in engineering, 1998, 43:1453 -1478

[7] Lin C.Y., Chao L.S．Automated image interpretation for integrated topology and shape optimization [J]. Structural and Multidisciplinary Optimization., 2000,20:125-137

[8] Tang P.S., Chang K.H．Integration of topology and shape optimization for design of structural components [J]. Structural and Multidisciplinary Optimization, 2001, 22: 65 – 82

[9] Jang G.W., Kim J.K., Kim Y.Y．Integrated topology and shape optimization software for compliant MEMS mechanism design[J].Engineering Software,2007,12(3): 1-14

[10] Li Zhao-kun, Zhang Xian-min, Huamei Bian, Xiaotie Niu. Multiobjective topology optimization of multiple inputs and outputs compliant mechanisms with geometrically nonlinearity [C], Advanced Materials Research ,2013, Vols. 706-708:pp. 864-877

[11] Li Zhao-kun, Huamei Bian, Lijuan Shi, Xiaotie Niu.MultiobjectiveTopology optimization of compliant mechanisms. Advanced Materials Research, 2014, Vols. 971-973:pp. 1941-1948

[12] Huang Jian-mei.Research on technology of data processing of the rapid reverse system based on deep image [D].Haer-bin: master degree of Haer-bin university of technology,2005